JOURNAL OF VIROLOGY, July 1999, p. 5605–5612 Vol. 73, No. 7
0022-538X/99/$04.00+0
Copyright © 1999, American Society for Microbiology. All Rights Reserved.

Mapping of Functional Elements in the Stem-Anchor Region of Tick-Borne Encephalitis Virus Envelope Protein E

STEVEN L. ALLISON,* KARIN STIASNY, KONRAD STADLER, CHRISTIAN W. MANDL, AND FRANZ X. HEINZ

Institute of Virology, University of Vienna, Vienna, Austria

Received 16 December 1998/Accepted 12 April 1999

Envelope protein E of the flavivirus tick-borne encephalitis virus mediates membrane fusion, and the structure of the N-terminal 80% of this 496-amino-acid-long protein has been shown to differ significantly from that of other viral fusion proteins. The structure of the carboxy-terminal 20%, the stem-anchor region, is not known. It contains sequences that are important for membrane anchoring, interactions with prM (the precursor of membrane protein M) during virion assembly, and low-pH-induced structural changes associated with the fusion process. To identify specific functional elements in this region, a series of C-terminal deletion mutants were constructed and the properties of the resulting truncated recombinant E proteins were examined. Full-length E proteins and proteins lacking the second of two predicted transmembrane segments were secreted in a particulate form when coexpressed with prM, whereas deletion of both segments resulted in the secretion of soluble homodimeric E proteins. Sites located within a predicted α-helical region of the stem (amino acids 431 to 449) and the first membrane-spanning region (amino acids 450 to 472) were found to be important for the stability of the prM-E heterodimer but not essential for prM-mediated intracellular transport and secretion of soluble E proteins. A separate site in the stem, also corresponding to a predicted α-helix (amino acids 401 to 413), was essential for the conversion of soluble protein E dimers to a homotrimeric form upon low-pH treatment, a process resembling the transition to the fusogenic state in whole virions. This functional mapping will aid in the understanding of the molecular mechanisms of membrane fusion and virus assembly.

Structural elements in the vicinity of the membrane anchor participate in a number of important functions of viral envelope proteins, including oligomerization, particle assembly, and membrane fusion. In orthomyxoviruses (5) and retroviruses (6, 7, 11, 29, 37, 39), structural data have suggested that α-helix-forming elements adjacent to the membrane-spanning segment play an important role in the extensive conformational changes that drive the fusion process, a feature that appears to be shared by the paramyxoviruses (24) and filoviruses (13, 38) as well.

Envelope protein E of tick-borne encephalitis (TBE) virus, a small enveloped virus belonging to the genus *Flavivirus* of the family *Flaviviridae*, has a structure and subunit organization fundamentally different from those of the examples mentioned above, even though the functions they perform are similar. The X-ray crystal structure (32) of a soluble ectodomain fragment of this protein has revealed that it is a head-to-tail dimer oriented parallel to the viral membrane, in contrast to most other viral fusion proteins studied so far, which are trimeric spikes. Another major difference is that the ectodomain fragment (sE dimer), representing the N-terminal 80% of the molecule, consists mostly of beta-sheet and loop structures and does not contain any long α-helical segments.

Although all of the known antigenic determinants, the putative receptor binding site, and the putative fusion peptide reside in the ectodomain portion of protein E (32), the remaining C-terminal 20% of this protein, referred to as the stem-anchor region, has also been shown to be important for a number of functions, including interactions with the precursor of membrane protein M (prM) during viral assembly (3), particle formation (3), and low-pH-induced structural changes associated with membrane fusion (36).

Newly synthesized E and prM proteins associate to form heterodimers (3, 40). These are incorporated into immature virions, which assemble in the endoplasmic reticulum and are transported via the secretory pathway (33). The intracellular virions remain in the immature form until shortly before release from the cell and then are converted to the active mature form by cleavage of prM by the cellular protease furin (35). Heterodimeric interactions between prM and E are important for proper transport and possibly folding of E (3, 25) and probably also for protection of the immature virion against acid inactivation during transport through acidic vesicles (14, 16, 19). Proper heterodimer interactions also appear to be required for the formation and secretion of subviral particles, which are capable of self-assembly in the absence of the nucleocapsid (3). These particles, which consist of native E and M proteins anchored in a lipid membrane (34), have been shown to have fusogenic properties similar to those of whole virions (10, 34).

Membrane fusion requires acidic pH and is mediated by protein E, which, in virions and recombinant subviral particles, is organized as a metastable network of interacting homodimers (2, 34). When exposed to acidic pH, the E dimers dissociate and reorganize irreversibly into a homotrimeric form (2), a process that appears to be required for fusion. Studies with protease-treated E proteins have suggested that elements within the stem-anchor are involved in the final formation of the E trimers, whereas the initial low-pH-dependent dissociation of the dimer occurs mainly within the ectodomain portion (36).

The stem-anchor region extends from the carboxy terminus of each of the monomers of the crystallized ectodomain fragment, placing it at the distal ends of the E homodimer (32). Although its structure has not been investigated experimen-

* Corresponding author. Mailing address: Institute of Virology, University of Vienna, Kinderspitalgasse 15, A-1095 Vienna, Austria. Phone: 43-1-404-90, ext. 79505. Fax: 43-1-406-21-61. E-mail: steven.allison@univie.ac.at.

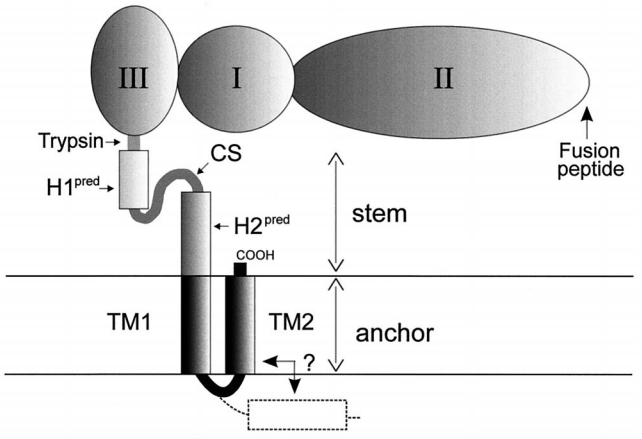

FIG. 1. Schematic diagram of a TBE virus protein E monomer (not to scale) which, in the native structure, forms a homodimer with a head-to-tail orientation. The three domains of the sE fragment (I, II, and III), which was cleaved from purified virions by trypsin and used previously for structure determination (32), are represented by shaded ovals, and the positions of the putative fusion peptide at the tip of domain II and the trypsin cleavage site next to domain III are indicated. The part below the trypsin cleavage site represents the C-terminal 20% of the E protein, for which only sequence-based structure predictions are available (36). The viral membrane is represented by parallel lines, and the portions of E corresponding to the stem and anchor regions are indicated. $H1^{pred}$ (residues 401 to 413) and $H2^{pred}$ (residues 431 to 449) indicate predicted α-helical regions in the stem, the CS element (residues 414 to 430) separates these putative helices, and TM1 (residues 450 to 471) and TM2 (residues 473 to 496) are predicted transmembrane segments (31). $H2^{pred}$ is contiguous with TM1, and these together may constitute a continuous α-helix with its C-terminal half spanning the viral membrane. TM2, which normally serves as the signal sequence for nonstructural protein NS1, is depicted as traversing the membrane, but it is not known whether it actually remains in the membrane after cleavage by signalase, which separates the E and NS1 proteins during processing of the viral polyprotein (33).

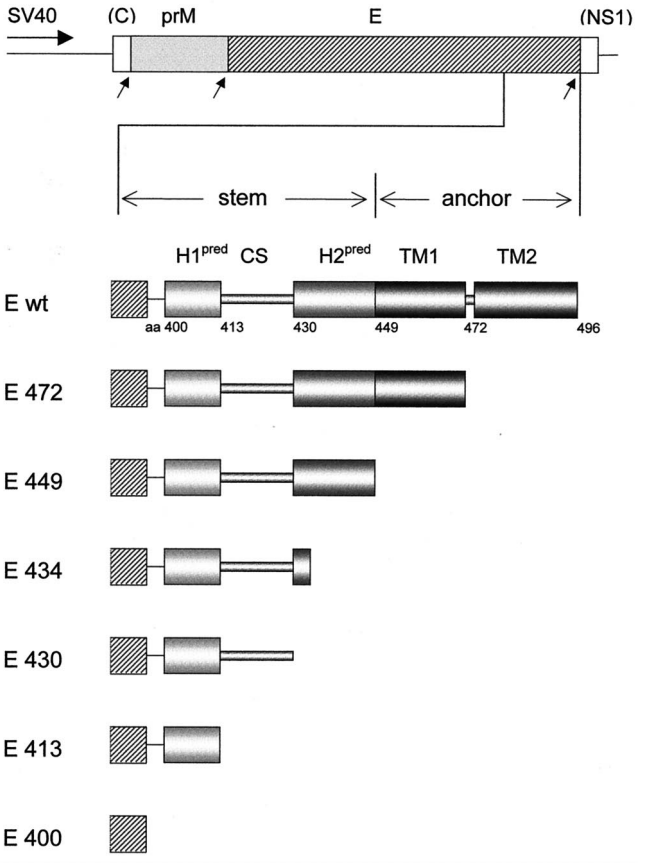

FIG. 2. C-terminal truncations in recombinant E proteins. The diagram shows the amino acid (aa) positions of the C-terminal truncations and which of the predicted structural elements of the stem-anchor region were present in each construct (Fig. 1 contains the definitions of the abbreviations). These proteins are designated by an E followed by the number of the last amino acid residue. The portion of the TBE genome containing the prM and E genes, cloned into a plasmid vector under the control of the SV40 early promoter (1), is shown at the top. Small arrows indicate the sites where the polyprotein is cleaved by signalase (33), and the short flanking sequences belonging to the C and NS1 coding regions are labeled.

tally, sequence-based predictions have allowed several potentially important structural elements to be identified (30, 36). As shown in Fig. 1, these include two predicted α-helical regions in the stem, a conserved sequence (CS) separating these predicted helices, and two predicted transmembrane segments in the anchor portion. In this study, we have used this information as the basis for constructing a series of C-terminally truncated E proteins and have used these constructs to identify specific regions that are important for interactions with prM, particle formation, and low-pH-induced structural changes.

MATERIALS AND METHODS

Plasmid construction and mutagenesis. Recombinant plasmids for coexpression of truncated E proteins with prM were derived from plasmid SV-PEwt (1), which contains cloned cDNA corresponding to nucleotides 388 to 2550 of the genome of TBE virus strain Neudoerfl (GenBank accession no. U27495). This construct includes the last 31 codons of the C gene, the entire prM and E genes, and the first 30 codons of the NS1 gene under the control of the simian virus 40 (SV40) early promoter (Fig. 2). It also contains an SV40 origin of replication for amplification in COS cells. Deletion mutants were constructed by replacing a *Sna*BI-*Not*I fragment (nucleotides 1881 to 2550) with a shorter PCR-generated fragment containing a TAG stop codon at the appropriate position, followed immediately by a *Not*I restriction site in place of the deleted sequence.

For expression of E400 without prM, the *Sna*BI-*Not*I fragment containing the C-terminal deletion was excised from the prM+E400 construct (Fig. 2) and inserted in place of the corresponding *Sna*BI-*Not*I fragment of plasmid SV-Ewt, which codes for protein E alone (1). The resulting plasmid contained nucleotides 883 to 2172 of the TBE virus genome and thus lacked all but the last 30 codons of the protein M coding region, which were retained to provide a signal sequence for protein E. Plasmid SV-prM, for expression of prM alone, was described previously (3).

Plasmids were propagated in *Escherichia coli* HB101 and purified by using a Qiagen Plasmid Mega Kit. The sequences of the PCR-generated portions, including the ligation junctions, were verified for each plasmid preparation before further use.

Expression, purification, and quantitation of E proteins. COS-1 cells (ATCC CRL 1659) were grown in Dulbecco's minimum essential medium (MEM; Life Technologies) supplemented with 10% fetal bovine serum, penicillin (100 U/ml), and streptomycin (100 μg/ml) at 37°C in 5% CO_2. Cells were transfected with purified plasmid by electroporation using a Bio-Rad Gene Pulser apparatus. The cell culture medium was replaced 22 h after transfection with serum-free bicarbonate- and HEPES-buffered Dulbecco's MEM (Life Technologies), and incubation was continued for 24 h until harvest. Cell culture supernatants were cleared by centrifugation at 10,000 rpm (16,000 × *g*) for 30 min at 4°C in a Sorvall F16/250 rotor, concentrated by ultrafiltration, and partially purified by centrifugation at 38,000 rpm for 20 h at 4°C in a 5 to 20% (wt/wt) sucrose gradient using a Beckman SW-40 rotor. For the pelleting experiments, the cleared supernatant was used without further treatment. The protein E concentration was determined by using a quantitative four-layer enzyme-linked immunosorbent assay (ELISA) after denaturation with sodium dodecyl sulfate (SDS) as described previously (19) by using SDS-treated virus or soluble protein E dimers (sE fragment) (18) as a standard. Hemagglutination (HA) activity was measured at pH 6.4 by the method of Clarke and Casals (9) with goose erythrocytes.

Metabolic labeling and immunoprecipitation. Cells were washed 41 h after transfection and incubated for 1 h at 37°C in methionine- and cysteine-free Dulbecco's MEM (Bio Whittaker). Labeling medium, consisting of the same medium with 1/20 of the normal concentration of unlabeled cysteine, [^{35}S]cysteine (Amersham), and the normal concentration of unlabeled methionine, was then applied to the cells, and labeling was continued for 6 h. After labeling, the cells were washed and lysed in a buffer consisting of 50 mM Tris-HCl (pH 8.0), 150 mM NaCl, 2 mM EDTA, 1% Triton X-100, 1 mM phenylmethylsulfonyl fluoride, and aprotinin at 2 μg/ml.

Lysates (70 μl) were precleared by using 2 μl of rabbit anti-mouse immuno-

globulin (Nordic) and 40 μl of a 50% slurry of protein A Sepharose (Pharmacia) in incubation buffer (20 mM Tris-HCl [pH 8.0], 150 mM NaCl, 2 mM EDTA, 0.5% Triton X-100, 1 mM phenylmethylsulfonyl fluoride, aprotinin at 2 μg/ml). The specific antibody (2 μl) and 2 μl of rabbit anti-mouse immunoglobulin were then added to the lysate, and the mixture was incubated for 30 min at room temperature. The protein A Sepharose slurry (40 μl) was then added, and incubation was continued for 1 h at room temperature with continuous, gentle rocking. Immunoprecipitates were collected by centrifugation and washed twice with incubation buffer, twice with incubation buffer containing 500 instead of 150 mM NaCl, and twice with 63 mM Tris-HCl (pH 6.8). The precipitated material was solubilized by heating for 5 min at 95°C in 40 μl of electrophoresis sample buffer (26) and analyzed by SDS-polyacrylamide gel electrophoresis (PAGE) and fluorography. Protein sizes were estimated by comparison to radiolabeled molecular weight standards (Amersham).

Chemical cross-linking, gel electrophoresis, and immunoblotting. Chemical cross-linking with dimethylsuberimidate (DMS) was done as described previously (2). The cross-linked proteins were separated by electrophoresis on 5% polyacrylamide gels using a continuous phosphate-buffered system as described by Maizel (28), blotted onto polyvinylidene difluoride membranes, and detected as described previously (35). The polyacrylamide gels used in the immunoprecipitation experiments were made by the method of Laemmli and Favre (26).

Low-pH treatment. For analysis of low-pH-induced changes, partially purified protein E preparations containing 0.5% Triton X-100 were acidified by adding the appropriate amount of a stock solution of 150 mM morpholineethanesulfonic acid (MES) and 0.5% Triton X-100 to yield a final pH of 6.0. The final protein E concentration of each sample was 40 μg/ml. The samples were incubated for 4 h at 25°C and then back-neutralized to pH 8.0 by using a stock solution of 150 mM triethanolamine and 0.5% Triton X-100.

Sedimentation analysis. For analysis of prM-E complexes, samples were applied to 5 to 20% (wt/wt) sucrose gradients made with 50 mM triethanolamine (pH 8.0), 100 mM NaCl, and 0.5% Triton X-100 and centrifuged for 22 h at 38,000 rpm and 15°C in a Beckman SW-40 rotor. Fractions of 0.6 ml were collected by upward displacement using an ISCO model 640 fraction collector and analyzed by immunoprecipitation and SDS-PAGE as described above.

For analysis of the oligomeric structure of soluble secreted E proteins, 7 to 20% (wt/wt) sucrose gradients containing 0.1% Triton X-100 were used and centrifugation was carried out for 20 h at 15°C. These samples were then analyzed by four-layer ELISA for protein E quantitation (19) or chemical cross-linking and gel electrophoresis (see above).

RESULTS

Construction of deletion mutants. To map the functionally important regions within the protein E stem-anchor region, we engineered a series of C-terminal deletions into wild-type expression plasmid SV-PEwt (1), which has been used previously for correct coexpression of prM and E proteins and production of recombinant subviral particles (3, 10, 17, 34). In each construct, a TAG stop codon was introduced at a position corresponding to the boundary of one of the predicted structural elements represented in Fig. 1 and the rest of the TBE virus-derived cDNA downstream from that site was deleted. The positions of the protein E truncations are shown in Fig. 2, with the number in the protein designation indicating the last amino acid before the stop codon (e.g., E472 consists of the first 472 amino acids of protein E). We truncated protein E472 after TM1, protein E449 after $H2^{pred}$, protein E430 after CS, protein E413 after $H1^{pred}$, and protein E400 before $H1^{pred}$. In addition, a previously described construct (SV-PEst) (1) containing a stop codon at position 435 but no deletion was used for coexpression of prM and E434, which is truncated within the $H2^{pred}$ element.

Interactions of truncated E proteins with prM. To examine the expression of the recombinant proteins and assess the requirements for formation of the prM-E heterodimer, the TBE virus proteins were expressed in COS-1 cells by transfection with the appropriate recombinant plasmid and the cells were metabolically labeled with [^{35}S]cysteine and lysed in a pH 8.0 buffer containing 1% Triton X-100. The proteins were then immunoprecipitated by using a monoclonal antibody (MAb) specific for either protein E (MAb A5) (15) or prM (MAb 8HI) (23) and analyzed by SDS-PAGE as shown in Fig. 3.

As expected, all of the C-terminally truncated E proteins were efficiently precipitated by MAb A5 (Fig. 3A), which is known to bind to a site in domain II of protein E (32). Each of the truncated E proteins was of the predicted size, indicating that proper processing had occurred. The full-length (wild-type) control, shown in Fig. 3A, was also of the predicted size, but in this particular sample an additional weaker band migrating more slowly than protein E could also be seen. This is possibly due to incomplete processing of the C-terminal end of full-length protein E, which terminates at a signalase cleavage site, rather than a stop codon (Fig. 2).

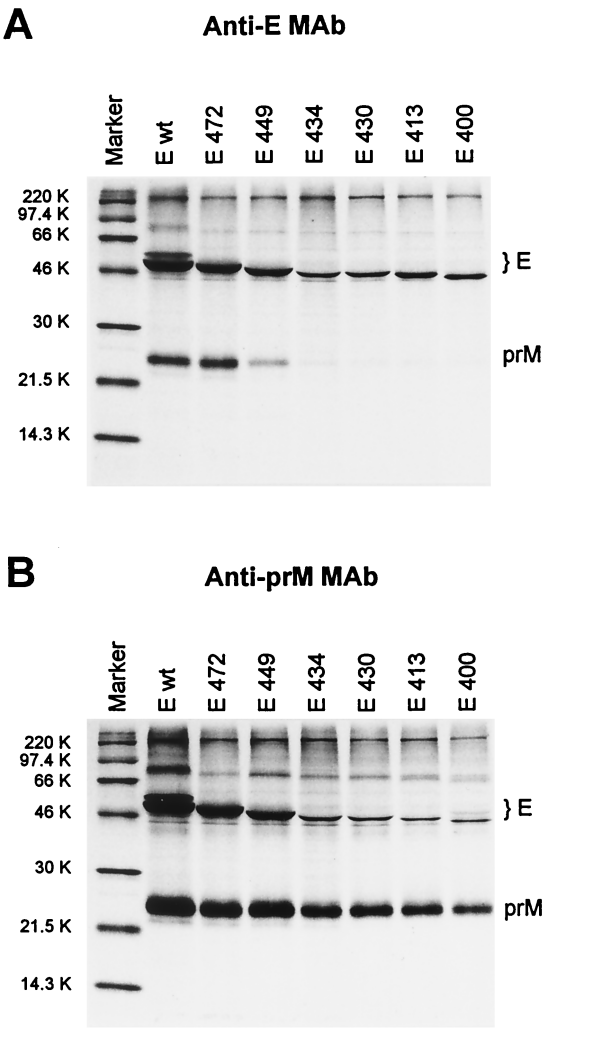

FIG. 3. SDS-PAGE of recombinant TBE virus proteins after immunoprecipitation with E-specific (A) and prM-specific (B) MAbs. COS cells were transfected with recombinant plasmids encoding prM together with one of the truncated forms of protein E shown in Fig. 2, radiolabeled, and lysed in a buffer containing 1% Triton X-100. The proteins were then immunoprecipitated, separated by SDS-PAGE, and visualized by fluorography. The values on the left are molecular weights.

Consistent with earlier results (3), full-length protein E (Ewt) and prM coexpressed in COS cells formed a detergent-stable heterodimer which could be immunoprecipitated by either protein E-specific MAb A5 (Fig. 3A) or prM-specific MAb 8HI (Fig. 3B). Some of the truncations, however, resulted in decreased efficiency of coprecipitation, suggesting that they had a direct influence on prM-E interactions. As shown in Fig. 3A, prM was efficiently coprecipitated with both Ewt and E472 when the protein E-specific MAb was used but the relative intensity of the prM band was somewhat weaker

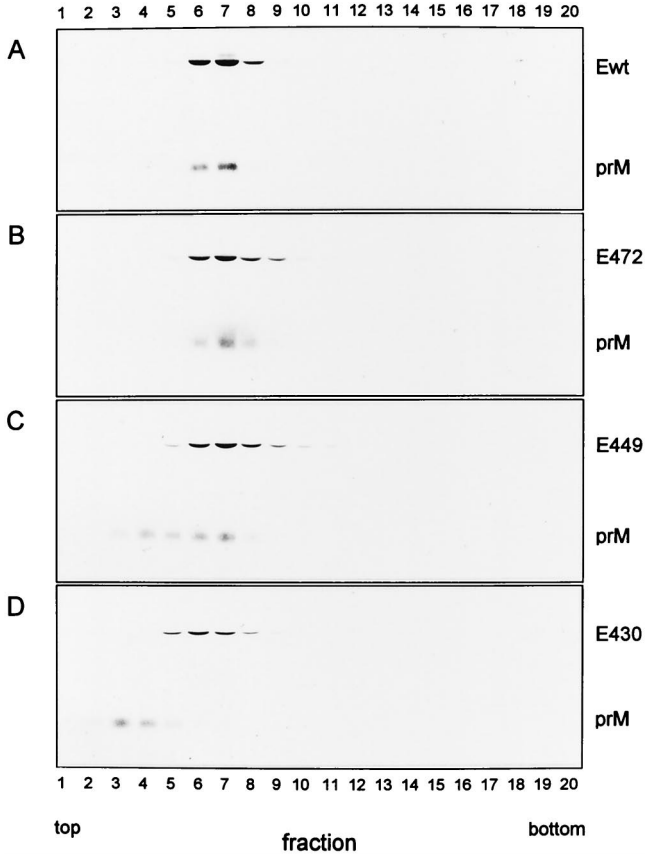

FIG. 4. Cosedimentation analysis of prM and truncated E proteins. The cell lysates used in the experiment depicted in Fig. 3 were analyzed by centrifugation in sucrose gradients (5 to 20%, wt/wt) containing 0.5% Triton X-100. Proteins were immunoprecipitated from the gradient fractions by using a polyclonal antiserum recognizing both prM and protein E, separated by SDS-PAGE, and visualized by fluorography. Panels: A, prM and Ewt; B, prM and E472; C, prM and E449; D, prM and E430. The sedimentation direction is left to right.

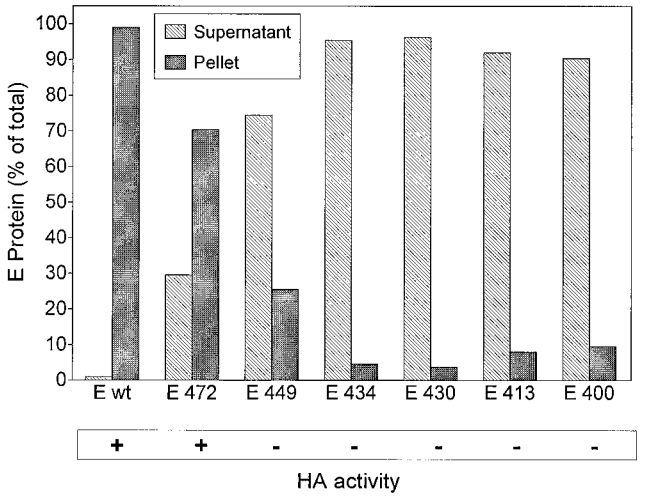

FIG. 5. Pelleting efficiencies and HA activities of secreted E proteins. Cleared supernatants from transfected COS cells were subjected to ultracentrifugation, and the amounts of protein E in the pellet and supernatant fractions after centrifugation were quantitated by ELISA. HA activity was determined both before and after pelleting. +, HA activity detected both before pelleting and in the pelleted fraction; −, no HA activity detected.

with E449 and much weaker still with E434, E430, E413, and E400. Immunoprecipitation of the same samples with a polyclonal antiserum recognizing both prM and protein E showed that the differences in prM band intensity were not due to differences in the relative level of protein expression (data not shown). Analogous results were obtained when a prM-specific MAb (8HI) was used instead to precipitate the prM-E complex (Fig. 3B); the relative efficiency of coprecipitation with prM was strong with Ewt and E472, intermediate with E449, and weak with E434, E430, E413, and E400.

To further investigate the stability of the prM-E complexes, the cell lysates used in the experiment whose results are shown in Fig. 3 were placed on sucrose gradients containing 0.5% Triton X-100 and sedimentation analysis was carried out to evaluate the degree to which prM remained associated with each of the truncated E proteins. As shown in Fig. 4A, prM and Ewt sedimented as a stable complex and the band intensity ratio for these two proteins was the same in each of the peak fractions. The sedimentation velocity of this complex was shown previously to correspond to a heterodimer containing one prM molecule and one protein E molecule (3). A similar pattern of cosedimentation was observed with the prM-E472 complex (Fig. 4B), consistent with the coimmunoprecipitation results. In contrast, the prM-E449 heterodimer, although clearly present in fractions 6 to 8, appeared to have partially dissociated during centrifugation, with some prM proteins at a higher position in the gradient (Fig. 4C). In the case of E430, the prM protein did not remain associated at all and the proteins were found in separate fractions (Fig. 4D). E434, E413, and E400 also failed to cosediment with prM under these conditions (data not shown). These data suggest that the $H2^{pred}$ element and the TM1 portion of protein E make an important contribution to the stability of the prM-E heterodimer.

Effect of truncations on the physical structure of secreted proteins. Analysis of cell culture supernatants revealed that all of the truncated E proteins were secreted together with the mature M protein and that the kinetics of protein E secretion were essentially identical for all of the constructs shown in Fig. 2 (data not shown). To assess the physical form of these proteins, cell supernatants that were harvested and cleared 48 h after transfection were subjected to ultracentrifugation and the amounts of protein E in the supernatant and pellet fractions were quantitated. As shown in Fig. 5, Ewt coexpressed with prM was found almost exclusively in the pellet fraction, which was expected because it had already been shown that this protein gets incorporated into 30-nm-diameter membrane-containing subviral particles (34). Of the truncated E proteins, E472 was the only one for which the majority of the material was found in the pellet fraction after centrifugation. This material, like the wild-type subviral particles, also possessed HA activity. These data suggest that E472 can also be incorporated into a subviral particle using only the TM1 segment as its membrane anchor. The other truncated E proteins (E449, E434, E430, E413, and E400), all of which lacked both of the predicted transmembrane segments, were present primarily in a soluble free form that remained in the supernatant fraction and did not possess any HA activity. Although E449 did tend to make a significant amount of pelletable material (Fig. 5), this material was found to consist of insoluble aggregates that were readily distinguishable from wild-type subviral particles by their different sedimentation properties and lack of HA activity (data not shown).

The oligomeric state of the soluble truncated forms of protein E (E449, E434, E430, E413, and E400) was then investi-

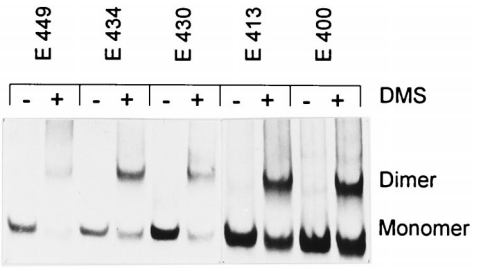

FIG. 6. Cross-linking analysis of soluble truncated E proteins. Partially purified E proteins were analyzed by SDS-PAGE and immunoblotting after treatment with the cross-linking reagent DMS. The positions of the protein E monomer and dimer bands are indicated. +, cross-linker added; −, no cross-linker.

gated by chemical cross-linking analysis. Cell supernatants were concentrated by ultrafiltration and treated with the bifunctional cross-linker DMS, which is known to form cross-links between the ectodomains of the protein E dimer (18). SDS-PAGE and immunoblotting of the DMS-treated proteins (Fig. 6) revealed that all of the extracellular soluble truncated E proteins were in the homodimeric state, demonstrating that the outer portion of the protein E ectodomain has the intrinsic ability to dimerize in the absence of the stem-anchor. Furthermore, all of these dimers yielded essentially identical reactivity profiles when tested in a four-layer ELISA system using a panel of MAbs recognizing different parts of protein E (data not shown). Therefore, the extent of the deletion in the stem-anchor did not appear to influence the overall folding of the protein E ectodomain.

Effect of truncations on prM-mediated secretion. Earlier experiments have shown that both full-length and C-terminally truncated E434 proteins require coexpression with prM for efficient secretion (3). It was therefore somewhat surprising that the elimination of $H2^{pred}$, which contributes to the stability of the prM-E heterodimer, did not seem to impair the ability of the soluble E proteins to be secreted. This suggests either that other interactions with prM outside the protein E stem-anchor region are used for prM-mediated transport and secretion or that the shorter forms of protein E do not require prM for secretion. To distinguish between these possibilities, a new plasmid construct encoding protein E400 but lacking the prM gene was made and this, together with a plasmid encoding prM alone, was used in a cotransfection experiment to assess the effect of prM on secretion.

As shown in Fig. 7, the efficiency of protein E400 secretion was drastically reduced when prM was omitted from the construct. The level of secretion could be partially restored, however, by providing prM in *trans* by cotransfection, demonstrating that prM is still capable of influencing the secretion of protein E even when the entire stem-anchor region is deleted. These data therefore suggest that there are further interactions between prM and the outer domains of protein E, separate from those in the stem region, that are involved in prM-mediated transport and secretion of protein E.

Effect of truncations on low-pH-induced structural changes. Earlier work has already revealed that protein E dimers dissociate and reorganize into homotrimers when exposed to low pH and that the stem-anchor region is important for the trimerization step (36). To map the location of a possible trimerization site in this region, we tested the abilities of the different soluble dimeric forms of protein E to undergo rearrangement into trimers after acid treatment. For these experiments, the truncated E proteins were first partially purified by sucrose gradient centrifugation in the absence of detergent. Under

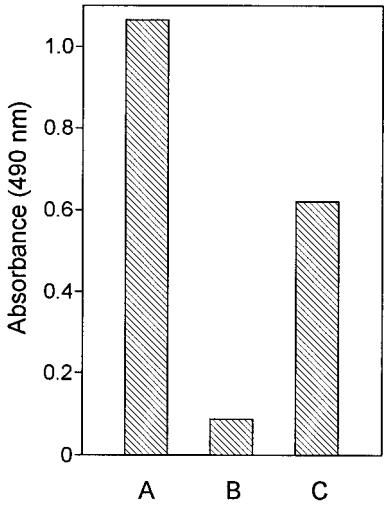

FIG. 7. Effect of coexpression with prM on E400 secretion efficiency. COS cells were transfected with expression plasmids encoding prM and E400 in the same construct (A), E400 alone (B), or prM and E400 on separate plasmids (C). At 29 h posttransfection, a protein E-specific four-layer ELISA (20) was used to detect secreted protein E in the supernatant. The transfection efficiency, as judged by immunofluorescence using a protein E-specific MAb, was the same (~50%) in all three samples (data not shown).

these conditions, the M proteins were removed as higher-molecular-weight complexes and the fractions containing the semipurified E proteins were judged by immunoblotting to be free of protein M (data not shown).

Protein E samples containing 0.5% Triton X-100 were treated at pH 6.0 (final protein E concentration, 40 μg/ml), back-neutralized to pH 8.0, and subjected to sedimentation analysis in a detergent-containing sucrose gradient to assess their oligomeric state. Full-length detergent-solubilized E proteins from TBE virus were used as a standard for comparison (36). As shown in Fig. 8A, treatment of solubilized full-length E proteins at low pH caused an irreversible conversion of dimers to trimers and the resulting shift in sedimentation velocity was identical to that observed previously when solubilized E proteins from low-pH-treated virions were used (2). Proteins E449, E434, E430, and E413 also clearly retained the ability to form trimers, and the sedimentation profile from the shortest of these, E413, is shown in Fig. 8B. The identities of the dimer and trimer peaks in these experiments were also confirmed by chemical cross-linking (Fig. 8A and B, insets).

In contrast to the longer forms, E400, which differs from E413 only by the lack of the 13-amino-acid-long $H1^{pred}$ element, was completely unable to form trimers under the conditions used, and after back-neutralization, only dimers were detected by both sedimentation analysis and cross-linking (Fig. 8C). Even when the E400 concentration during the incubation at low pH was increased to 80 μg/ml, no trimerization could be detected (data not shown). If the sample was not back-neutralized, however, and the sedimentation analysis was carried out at pH 6.0, the E400 protein sedimented as a monomer (data not shown), as has been shown previously with E proteins whose stem-anchor region had been proteolytically removed (36). This indicates that the E400 dimer undergoes a reversible dissociation in response to low-pH treatment but, due to the lack of the $H1^{pred}$ element, does not assemble into the trimeric form.

Although E449, E434, E430, and E413 were efficiently converted to trimers at low pH, monomeric forms could be de-

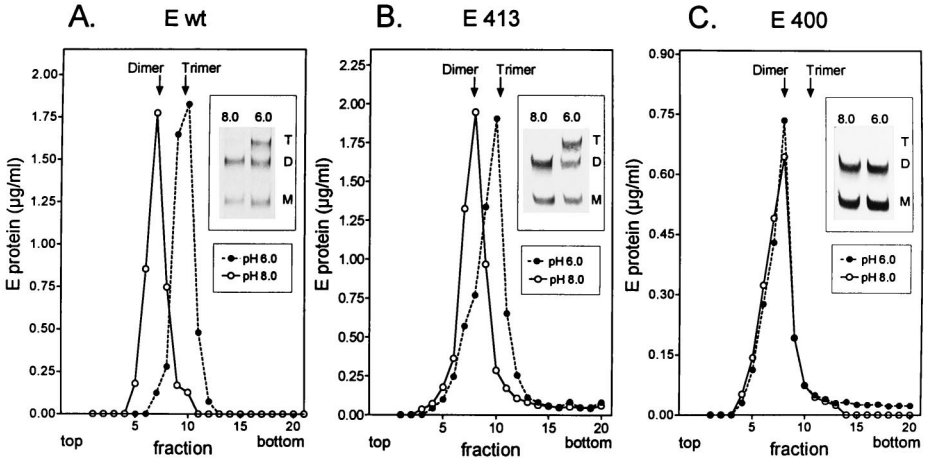

FIG. 8. Sedimentation analysis of detergent-solubilized E proteins at pH 8.0 (solid curves) or after pretreatment at pH 6.0 and back-neutralization to pH 8.0 (dashed curves). Samples were centrifuged in sucrose gradients (7 to 20%, wt/wt) containing 0.1% Triton X-100, and the amount of protein E in each fraction was quantitated by ELISA. For the insets, material from the peak fractions was subjected to DMS cross-linking and immunoblotting as described in the legend to Fig. 6. M, monomer; D, dimer; T, trimer.

tected under conditions that were kinetically unfavorable for trimerization in solution, e.g., a lower protein E concentration (2 μg/ml) (data not shown). This is consistent with a two-step trimerization mechanism (36) in which the truncated protein E dimers first dissociate in response to low pH and then, if the $H1^{pred}$ element is present, reassociate in a subsequent step to create the trimeric form.

DISCUSSION

The results of this study allow fine mapping of functionally important elements within the C-terminal 20% of TBE virus protein E and also provide new information about functions that are independent of the stem-anchor region. A summary is provided in Table 1.

Domains I, II, and III (ectodomain). The ectodomain, defined here as the entire portion preceding the stem-anchor, consists of approximately the first 400 amino acids of protein E, and its three-dimensional structure has been solved by X-ray crystallography (32). It is composed of three separate structural domains (designated I, II, and III), which contain all of the known antigenic determinants, as well as the putative receptor-binding site and fusion peptide. All three of these domains participate in homodimeric contacts between the E monomers, and the dimeric state is preserved when the ectodomain fragment is removed from the virion by limited trypsin digestion (18, 32). The present study demonstrated that C-terminally truncated recombinant E proteins lacking part or all of the stem-anchor are secreted in a dimeric form, indicating that the known contacts between the ectodomains are sufficient not only for maintenance of the dimeric state but also for initial formation of the E dimer in vivo. The ectodomain contacts are pH sensitive, and both recombinant protein E400 and the viral ectodomain fragment obtained by trypsin cleavage (36) dissociate in a reversible manner when exposed to low pH. This suggests that the acid-sensitive trigger for the fusion reaction resides in the ectodomain rather than in the stem.

TABLE 1. Functions of structural elements of TBE virus protein E

Amino acids	Sequence element(s)	Functional property(ies)
1–400	Domains I, II, III	Antigenic determinants, putative receptor-binding site, interactions with target membrane for fusion, contacts for homodimer formation, interactions with prM required for secretion, trigger for low-pH-induced dissociation
401–413	$H1^{pred}$	Trimerization of soluble protein E
414–430	CS	Unknown
431–449	$H2^{pred}$	Stabilization of prM-E interactions (not required for secretion)
450–472	TM1	Membrane anchor (needed for incorporation of protein E into particles), stabilization of prM-E interactions
473–496	TM2	Signal sequence for NS1 (not essential for particle formation)

In contrast to the protein E homodimer interactions, the heterodimeric interactions between prM and protein E appear to involve both the ectodomain and the stem-anchor. Indirect evidence based on comparison of antibody binding to mature and immature flaviviruses (14, 19) has suggested that domain II of the protein E ectodomain is involved in these contacts (32). Our observation that coexpression with prM enhances the efficiency of secretion of E proteins lacking the entire stem-anchor provides further indirect evidence that prM associates with the ectodomain of protein E and that these interactions are of particular importance for the efficient transport of protein E.

The stem. An important finding of this study is that a predicted α-helical element in the stem, $H1^{pred}$ (amino acids 401 to 413) appears to be involved in the formation of protein E homotrimers in solution upon low-pH treatment. Proteins lacking this sequence and the rest of the stem-anchor are still secreted in a dimeric form that dissociates at low pH but does not go on to form trimers. In contrast, E proteins that were truncated immediately after the $H1^{pred}$ element could be irreversibly converted by low-pH treatment to the trimeric form. It is therefore likely that residues within this element either are directly involved in trimeric contacts between the subunits of the low-pH form of protein E or facilitate the conversion of monomers into trimers.

Unexpectedly, our data did not reveal a function for the CS

element (amino acids 414 to 430), the part of the stem that is most highly conserved among flaviviruses (36). Although its high degree of conservation (8 of 17 residues are invariable) implies an important function, it does not seem to be directly involved in homodimeric or trimeric interactions between the E proteins or heteromeric interactions with prM.

The $H2^{pred}$ element (amino acids 431 to 449) and the TM1 element (amino acids 450 to 472) were found to be important for the stability of the prM-E dimer and therefore may interact directly with prM. The weakening of the prM-E interaction by the deletion of TM1, however, could also be due to a general destabilizing effect on $H2^{pred}$ caused by the truncation of a putative continuous α-helix extending through both $H2^{pred}$ and TM1 (36).

The anchor. The predicted transmembrane elements TM1 and TM2 lie at the extreme C-terminal end of protein E and are predicted to constitute a double membrane anchor (30). It was revealed by sequential deletion that the second of these (TM2, amino acids 473 to 496) is dispensable for the incorporation of protein E into recombinant subviral particles, whereas E proteins with both segments deleted are secreted as free homodimers when coexpressed with prM. Since the TM2 element serves as a signal sequence for the nonstructural protein NS1 during flavivirus protein synthesis (33), it is possible that it has no further functional role in mature protein E, although it is still likely to make a contribution to the overall structural organization of the virion.

Functional role of the stem region. In contrast to most of the viral fusion proteins that have been studied so far, which are trimeric in both the native and fusogenic states (21), the detergent-stable form of TBE virus protein E is a homodimer in its native state but is irreversibly converted to a trimeric form at the pH of fusion (2). We demonstrate here that recombinant protein E dimers expressed in COS cells are capable of undergoing this transformation in solution when exposed to low pH and that the other viral membrane protein, M, is not required for this process.

From the head-to-tail orientation of the sE dimer, it is predicted that the stem regions of the two subunits would not interact with each other in the neutral form, since they extend down from the distal ends of the dimer and are therefore separated by a distance of several nanometers (32). Recently, however, we presented a model in which direct interactions between the stem regions of adjacent protein E subunits on the virion surface are proposed to be responsible for the formation of trimers at low pH (36). The present data are consistent with this model, but it cannot yet be concluded whether the stem regions actually make contact with each other in the trimeric state or whether other portions of the molecule are involved.

The $H1^{pred}$ element has been predicted to be a 13-amino-acid-long amphipathic α-helix (36) and, by analogy to the fusogenic proteins of other enveloped viruses (4, 5–7, 11, 12, 24, 27, 29, 37–39), might be expected to participate in the formation of a trimeric core structure during the membrane fusion process. This analogy, however, is severely limited by the fact that TBE virus protein E does not appear to have the potential to form long coiled coils of α-helices, a central feature of the general model that is now emerging for other viral fusion proteins (8, 22, 39). It is therefore likely that not only the role of the stem region but also the overall mechanism leading to membrane fusion might differ significantly from the established paradigm, with flavivirus protein E representing a different structural class of fusion protein. Further studies carried out in the presence of target membranes are necessary in order to relate structural changes to the membrane fusion event itself, but the mapping results shown here should provide important clues regarding the possible roles of specific structures in this process.

ACKNOWLEDGMENTS

We thank Melby Wilfinger, Angela Dohnal, and Walter Holzer for technical assistance; Regina Kofler for help with plasmid construction; and C. S. Schmaljohn, USAMRIID, Ft. Detrick, Md., for providing MAb 8HI.

Part of this work was supported by a grant from the International Human Frontier Science Program.

REFERENCES

1. **Allison, S. L., C. W. Mandl, C. Kunz, and F. X. Heinz.** 1994. Expression of cloned envelope protein genes from the flavivirus tick-borne encephalitis virus in mammalian cells and random mutagenesis by PCR. Virus Genes **8:**187–198.
2. **Allison, S. L., J. Schalich, K. Stiasny, C. W. Mandl, C. Kunz, and F. X. Heinz.** 1995. Oligomeric rearrangement of tick-borne encephalitis virus envelope proteins induced by an acidic pH. J. Virol. **69:**695–700.
3. **Allison, S. L., K. Stadler, C. W. Mandl, C. Kunz, and F. X. Heinz.** 1995. Synthesis and secretion of recombinant tick-borne encephalitis virus protein E in soluble and particulate form. J. Virol. **69:**5816–5820.
4. **Blacklow, S. C., M. Lu, and P. S. Kim.** 1995. A trimeric subdomain of the simian immunodeficiency virus envelope glycoprotein. Biochemistry **34:** 14955–14962.
5. **Bullough, P. A., F. M. Hughson, J. J. Skehel, and D. C. Wiley.** 1994. Structure of influenza haemagglutinin at the pH of membrane fusion. Nature **371:**37–43.
6. **Caffrey, M., M. Cai, J. Kaufman, S. J. Stahl, P. T. Wingfield, D. G. Covell, A. M. Gronenborn, and G. M. Clore.** 1998. Three-dimensional solution structure of the 44 kDa ectodomain of SIV gp41. EMBO J. **17:**4572–4584.
7. **Chan, D. C., D. Fass, J. M. Berger, and P. S. Kim.** 1997. Core structure of gp41 from the HIV envelope glycoprotein. Cell **89:**263–273.
8. **Chan, D. C., and P. S. Kim.** 1998. HIV entry and its inhibition. Cell **93:**681–684.
9. **Clarke, D. H., and J. Casals.** 1958. Techniques for hemagglutination and hemagglutination inhibition with arthropod-borne viruses. Am. J. Trop. Med. Hyg. **7:**561–573.
10. **Corver, J., A. Ortiz, S. L. Allison, J. Schalich, F. X. Heinz, and J. Wilschut.** Membrane fusion activity of tick-borne encephalitis (TBE) virus and recombinant subviral particles (RSPs) in a liposomal model system. Submitted for publication.
11. **Fass, D., S. C. Harrison, and P. S. Kim.** 1996. Retrovirus envelope domain at 1.7 Angstrom resolution. Nat. Struct. Biol. **3:**465–469.
12. **Fass, D., and P. S. Kim.** 1995. Dissection of a retrovirus envelope protein reveals structural similarity to influenza hemagglutinin. Curr. Biol. **5:**1377–1383.
13. **Gallaher, W. R.** 1996. Similar structural models of the transmembrane proteins of Ebola and avian sarcoma viruses. Cell **85:**477–478.
14. **Guirakhoo, F., R. A. Bolin, and J. T. Roehrig.** 1992. The Murray Valley encephalitis virus prM protein confers acid resistance to virus particles and alters the expression of epitopes within the R2 domain of E glycoprotein. Virology **191:**921–931.
15. **Guirakhoo, F., F. X. Heinz, and C. Kunz.** 1989. Epitope model of tick-borne encephalitis virus envelope glycoprotein E: analysis of structural properties, role of carbohydrate side chain, and conformational changes occurring at acidic pH. Virology **169:**90–99.
16. **Guirakhoo, F., F. X. Heinz, C. W. Mandl, H. Holzmann, and C. Kunz.** 1991. Fusion activity of flaviviruses: comparison of mature and immature (prM-containing) tick-borne encephalitis virions. J. Gen. Virol. **72:**1323–1329.
17. **Heinz, F. X., S. L. Allison, K. Stiasny, J. Schalich, H. Holzmann, C. W. Mandl, and C. Kunz.** 1995. Recombinant and virion-derived soluble and particulate immunogens for vaccination against tick-borne encephalitis. Vaccine **13:**1636–1642.
18. **Heinz, F. X., C. W. Mandl, H. Holzmann, C. Kunz, B. A. Harris, F. Rey, and S. C. Harrison.** 1991. The flavivirus envelope protein E: isolation of a soluble form from tick-borne encephalitis virus and its crystallization. J. Virol. **65:** 5579–5583.
19. **Heinz, F. X., K. Stiasny, G. Püschner-Auer, H. Holzmann, S. L. Allison, C. W. Mandl, and C. Kunz.** 1994. Structural changes and functional control of the tick-borne encephalitis virus glycoprotein E by the heterodimeric association with protein prM. Virology **198:**109–117.
20. **Heinz, F. X., W. Tuma, F. Guirakhoo, and C. Kunz.** 1986. A model study of the use of monoclonal antibodies in capture enzyme immunoassays for antigen quantification exploiting the epitope map of tick-borne encephalitis virus. J. Biol. Stand. **14:**133–141.
21. **Hernandez, L. D., L. R. Hoffman, T. G. Wolfsberg, and J. M. White.** 1996. Virus-cell and cell-cell fusion. Annu. Rev. Cell Dev. Biol. **12:**627–661.
22. **Hughson, F. M.** 1997. Enveloped viruses: a common mode of membrane fusion? Curr. Biol. **7:**R565–R569.

23. **Iacono-Connors, L. C., J. F. Smith, T. G. Ksiazek, C. L. Kelley, and C. S. Schmaljohn.** 1996. Characterization of Langat virus antigenic determinants defined by monoclonal antibodies to E, NS1 and preM and identification of a protective, non-neutralizing preM-specific monoclonal antibody. Virus Res. **43:**125–136.
24. **Joshi, S. B., R. E. Dutch, and R. A. Lamb.** 1998. A core trimer of the paramyxovirus fusion protein: parallels to influenza virus hemagglutinin and HIV-1 gp41. Virology **248:**20–34.
25. **Konishi, E., and P. W. Mason.** 1993. Proper maturation of the Japanese encephalitis virus envelope glycoprotein requires cosynthesis with the premembrane protein. J. Virol. **67:**1672–1675.
26. **Laemmli, U. K., and M. Favre.** 1973. Maturation of the head of bacteriophage T4. I. DNA packaging events. J. Mol. Biol. **80:**575–599.
27. **Lu, M., S. C. Blacklow, and P. S. Kim.** 1995. A trimeric structural domain of the HIV-1 transmembrane glycoprotein. Nat. Struct. Biol. **2:**1075–1082.
28. **Maizel, J. V., Jr.** 1971. Polyacrylamide gel electrophoresis of viral proteins. Methods Virol. **5:**179–246.
29. **Malashkevich, V. N., D. C. Chan, C. T. Chutkowski, and P. S. Kim.** 1998. Crystal structure of the simian immunodeficiency virus (SIV) gp41 core: conserved helical interactions underlie the broad inhibitory activity of gp41 peptides. Proc. Natl. Acad. Sci. USA **95:**9134–9139.
30. **Mandl, C. W., F. Guirakhoo, H. Holzmann, F. X. Heinz, and C. Kunz.** 1989. Antigenic structure of the flavivirus envelope protein E at the molecular level, using tick-borne encephalitis virus as a model. J. Virol. **63:**564–571.
31. **Mandl, C. W., F. X. Heinz, and C. Kunz.** 1988. Sequence of the structural proteins of tick-borne encephalitis virus (Western subtype) and comparative analysis with other flaviviruses. Virology **166:**197–205.
32. **Rey, F. A., F. X. Heinz, C. Mandl, C. Kunz, and S. C. Harrison.** 1995. The envelope glycoprotein from tick-borne encephalitis virus at 2 Å resolution. Nature **375:**291–298.
33. **Rice, C. M.** 1996. Flaviviridae: the viruses and their replication, p. 931–959. *In* B. N. Fields, D. N. Knipe, P. M. Howley, R. M. Chanock, J. L. Melnick, T. P. Monath, B. Roizman, and S. E. Straus (ed.), Virology, 3rd ed. Lippincott-Raven, Philadelphia, Pa.
34. **Schalich, J., S. L. Allison, K. Stiasny, C. W. Mandl, C. Kunz, and F. X. Heinz.** 1996. Recombinant subviral particles from tick-borne encephalitis virus are fusogenic and provide a model system for studying flavivirus envelope glycoprotein functions. J. Virol. **70:**4549–4557.
35. **Stadler, K., S. L. Allison, J. Schalich, and F. X. Heinz.** 1997. Proteolytic activation of tick-borne encephalitis virus by furin. J. Virol. **71:**8475–8481.
36. **Stiasny, K., S. L. Allison, A. Marchler-Bauer, C. Kunz, and F. X. Heinz.** 1996. Structural requirements for low-pH-induced rearrangements in the envelope glycoprotein of tick-borne encephalitis virus. J. Virol. **70:**8142–8147.
37. **Tan, K., J.-H. Liu, J.-H. Wang, S. Shen, and M. Lu.** 1997. Atomic structure of a thermostable subdomain of HIV-1 gp41. Proc. Natl. Acad. Sci. USA **94:**12303–12308.
38. **Weissenhorn, W., L. J. Calder, S. A. Wharton, J. J. Skehel, and D. C. Wiley.** 1998. The central structural feature of the membrane fusion protein subunit from the Ebola virus glycoprotein is a long triple-stranded coiled coil. Proc. Natl. Acad. Sci. USA **95:**6032–6036.
39. **Weissenhorn, W., A. Dessen, S. C. Harrison, J. J. Skehel, and D. C. Wiley.** 1997. Atomic structure of the ectodomain from HIV-1 gp41. Nature **387:**426–430.
40. **Wengler, G., and G. Wengler.** 1989. Cell-associated West Nile flavivirus is covered with E+Pre-M protein heterodimers which are destroyed and reorganized by proteolytic cleavage during virus release. J. Virol. **63:**2521–2526.